TELKOMNIKA Indonesian Journal of Electrical Engineering
Vol. 12, No. 12, December 2014, pp. 8217 ~ 8228
DOI: 10.11591/telkomnika.v12i12.4640

Chaotic Binary Modulation Excitation Sequences for Multichannel Ultrasonic Ranging System

Yao Zhenjing, Yang Jingsong
Department of Disaster Prevention Instrument, Institute of Disaster Prevention,
Sanhe Hebei, 065201, China

Abstract

Ultrasonic crosstalk often causes false time-of-flight (TOF) in distance measurement. The excitation sequences with good correlation characteristics, i.e., sharp autocorrelation and flat cross-correlation, can help avoid crosstalk between multichannel ultrasonic sensors. A crosstalk elimination method by using the optimal binary excitation sequences modulated with chaotic codes, which includes chaotic binary amplitude shift keying (c-BASK), chaotic binary phase shift keying (c-BPSK) and chaotic binary frequency shift keying (c-BFSK), is proposed in this paper. The selection of the optimal chaotic initial values with the best echo correlation characteristics is realized by adopting a genetic algorithm. A square wave is used as the carrier of the chaotic binary modulation methods in order to reduce hardware cost. However, it could suffer from the decreased energy efficiency caused by mismatching spectrum with ultrasonic ranging system. The parameters of the chaotic binary modulation methods are configured to make their central frequency and bandwidth matched with that of the ultrasonic ranging system very well. Experiments have been conducted using an ultrasonic ranging system that consists of eight-channel SensComp 600 series instrument-grade electrostatic sensors excited with chaotic binary sequences. Experimental results show that the c-BFSK outperforms the c-BASK and c-BPSK in terms of the energy efficiency, e.g., 0.3508ζ vs. 0.3365ζ and 0.3279ζ, respectively. And the optimized c-BFSK sequence also has the best echo correlation characteristics among the chaotic binary modulation sequences.

Keywords: *ultrasonic crosstalk, binary modulation, chaotic series, energy efficiency, correlation characteristic*

1. Introduction

Ultrasonic sensors have been extensively applied on rescue robot for distance measurements, thanks to their low price and simple hardware interface. To obtain 360-degree panorama distance information, multichannel ultrasonic sensors composing a ring are required in a rescue robot [1]. One problem with these simultaneously working sensors in a ring is ultrasonic crosstalk, in which one ultrasonic sensor receives echo transmitted by another ultrasonic sensor [2]. Generally, ultrasonic receiver cannot distinguish whether the received echo from its own transmission or not, so the incorrect time-of-flight (TOF) measurements often occur.

The effective crosstalk elimination method is to give each ultrasonic sensor a unique excitation signature in the transmission and then identify the signature using a correlation technique in the receiver. Jörg and Berg [3] were the first to give a recognizable signature of each sensor in the transmission using pseudorandom code and frequency modulation. And then in the receiving circuit, the identification of the transmitted source sensor was by a matched filter. Subsequently, some researchers have applied different codes and modulation schemes to construct excitation sequences as a transmission signature to solve the ultrasonic crosstalk problem. Barker codes [4] were used to avoid crosstalk in ultrasonic system, although the available Barker codes limit their application. In ultrasonic distance measurement system, Golay codes [5-7] were applied to restrain crosstalk and increase the signal-to-noise ratio. But the realization complexity of Golay codes restricts their application. The binary-coded frequency shift keying (BFSK) signal and binary-coded phase shift keying (BPSK) signal [8] were applied to drive multiple piezoelectric ultrasonic sensors with narrow bandwidth. In reference [9] and [10], BPSK modulation was both used to construct the transmission signals of ultrasonic system. But they adopted different codes to modulate, i.e., Alvarez *et al*. [9] used complementary sequences codes and Iwasawa *et al*. [10] applied M sequence. Chaotic codes having sharp autocorrelation

Received October 10, 2013; Revised September 10, 2014; Accepted October 19, 2014

function and flat cross-correlation function are sensitive to small changes in the initial conditions and in parameter values. Therefore, Fortuna *et al*. [11] exploited chaotic pulse position modulation (CPPM) to excite the ultrasonic sensor to eliminate crosstalk and improve the efficiency of ultrasonic system. Yao *et al*. [12] proposed chaotic pulse position–width modulation (CPPWM) sequences to construct short digital excitation sequences to trigger ultrasonic sensors. Meng *et al*. [13] used a genetic algorithm (GA) to optimize short CPPM and pseudorandom PPM triggering sequences in order to minimize the maximal side-lobe of autocorrelation and the peak of cross-correlation function.

As we know, ultrasonic sensors work like band-pass filters and have bell-shaped magnitude spectrum. If the spectrum of the excited sequence does not match that of the ultrasonic sensor, some of the excitation energy cannot be transmitted by the ultrasonic system which decreases the energy efficiency. Pollatowski and Ermert [14] used transmitter signals with a constant amplitude level and nonlinear frequency modulation to match the spectrum of their ultrasonic system. Meng *et al*. [15] adopted spectrum optimization of a CPPM excitation sequence to improve energy efficiency. Yao *et al*. [12] used nondominated sorting genetic algorithm II to optimize both pulse periods and duty ratio of the CPPWM excitation sequences in order to maximize echo energy simultaneously on the basis of a best correlation characteristics.

To our knowledge, not many researchers discuss rejecting crosstalk in a multichannel ultrasonic ranging system based on the binary excitation sequences modulated with chaotic codes to drive electrostatic sensors. Moreover, fewer researchers debate the parameters configuration method for binary modulation excitation sequences to make their central frequency and bandwidth matched that of the ultrasonic system. This paper aims to exploit the novel crosstalk elimination method by applying chaotic binary modulation excitation sequences which includes chaotic binary amplitude shift keying (c-BASK), chaotic binary phase shift keying (c-BPSK), and chaotic binary frequency shift keying (c-BFSK). A square wave is used as the carrier wave of the chaotic binary modulation methods in order to reduce hardware cost. However, it could suffer from the decreased energy efficiency caused by mismatching spectrum with ultrasonic system. To improve energy efficiency, the parameters of the chaotic binary modulation methods are configured to make their central frequency and bandwidth matched that of the ultrasonic system very well. The chaotic initial values are optimized by applying GA to achieve the optimal correlation characteristics. The ultrasonic system that consists of eight-channel SensComp 600 series instrument-grade electrostatic sensors was designed and recommended the best chaotic binary modulation approach for electrostatic ultrasonic sensor via experiments.

The remainder of this paper is organized as follows. Section II presents the principle of chaotic binary modulation excitation sequence. The correlation characteristics and energy efficiency are explained in section III. Section IV introduces the parameter configuration methods of the binary modulation and the GA-based optimization of the excitation sequences. Section V shows the experiments and discussion, followed by the conclusions in section VI.

2. The Principle of Chaotic Binary Modulation Excitation Sequence

2.1. Chaotic Codes

Chaotic codes had been used to construct excitation sequence because of their good correlation characteristics (i.e. sharp autocorrelation function and flat cross-correlation function). Moreover, they are sensitive to small changes in the initial conditions and in parameter values. In this paper, the Ulam–von Neumann transformation [16] was used to generate chaotic codes as follows:

$$y_i = 1 - 2y_{i-1}^2, y_i \in [-1,1],\ i = 1,2,\ldots \tag{1}$$

Binary chaotic codes were generated by the following formula,

$$\mathrm{sgn}(y_i) = \begin{cases} 0 & y_i < 0 \\ 1 & y_i \geq 0 \end{cases}, i = 1,2,\ldots \tag{2}$$

2.2. Binary Modulation Scheme

The binary modulation techniques include binary amplitude shift keying (BASK), binary frequency shift keying (BFSK) and binary phase shift keying (BPSK), which have two states of amplitude, frequency and phase, respectively. In the proposed chaotic binary modulation approach, the variation of amplitude, frequency and phase are on the basis of chaotic codes.

2.2.1. Determination of carrier signal

In traditional approach, a sinusoidal signal is generally used as the carrier signal of the binary modulation technique. Since the hardware implementation of a square wave is much easier than a sinusoidal wave, the following square wave $q(t)$ is adopted as the carrier signal of chaotic binary modulation sequences,

$$q(t)=\begin{cases}1 & nT_c \le t < (n+1/2)T_c \\ 0 & (n+1/2)T_c \le t \le (n+1)T_c\end{cases}, n=0,\pm1,\pm2,\ldots, \quad (3)$$

Where T_c is the period of the square wave.

The square wave $q(t)$ can be represented as a Fourier series,

$$q(t)=\frac{1}{2}+\sum_{k=0}^{\infty}\frac{2}{\pi(2k+1)}\sin\left[\frac{2\pi(2k+1)}{T_c}t\right] \quad . \quad (4)$$

From the above expression, we can find that the square wave is a composite of a direct-current component and odd harmonic components. In all of the odd harmonic components, the energy of the fundamental harmonic is the highest. Because the ultrasonic system works as a pass-band filter, only the odd harmonic components within the pass-band of the ultrasonic system are received. Therefore, to obtain the highest energy efficiency, the spectrum of fundamental harmonic must match with that of the ultrasonic system.

2.2.2. c-BASK

In BASK, the amplitude of a fixed-frequency carrier wave is changed with each symbol of base-band signal. For the c-BASK, the binary chaotic codes were used as the base-band signal. Mathematically, the form for c-BASK sequence can be written as:

$$X_{BASK}(t)=c(t)\left\{\frac{1}{2}+\sum_{k=0}^{\infty}\frac{2}{\pi(2k+1)}\sin\left[\frac{2\pi(2k+1)}{T_c}t\right]\right\}, \quad (5)$$

Where $c(t)$ is binary chaotic codes used to change the amplitude of carrier signal. And the value of $c(t)$ is either 1 or 0.

2.2.3. c-BPSK

In BPSK, the phase of a constant amplitude and frequency carrier signal alters between zero and π. The symbols “1” and “0” are represented by zero and π of carrier signal, respectively. With c-BPSK, the chaotic information is contained in the instantaneous phase of the modulated carrier signal. The c-BPSK is given by the following formula:

$$X_{BPSK}(t)=\frac{1}{2}+\sum_{k=0}^{\infty}\frac{2}{\pi(2k+1)}\sin\left\{\frac{2\pi(2k+1)}{T_c}t+[1-c(iT_s)]\pi\right\} \quad (6)$$

Where T_s is the symbol width of base-band signal. In c-BPSK, the base-band signal is the binary chaotic codes.

2.2.4. c-BFSK

BFSK transmits the information using different carrier frequencies to represent symbol states. The amplitude remains unchanged. In BFSK, the symbols “1” and “0” are represented by

the carrier frequencies f_1 and f_2, respectively. For the *c*-BFSK, the value of binary chaotic codes, either 1 or 0, is determined using (1) and (2). Mathematically this is written by the following:

$$X_{BFSK}(t)=\begin{cases}\frac{1}{2}+\sum_{k=0}^{\infty}\frac{2}{\pi(2k+1)}\sin\left[2\pi(2k+1)f_1t\right], c(t)=1\\ \frac{1}{2}+\sum_{k=0}^{\infty}\frac{2}{\pi(2k+1)}\sin\left[2\pi(2k+1)f_2t\right], c(t)=0\end{cases} \quad (7)$$

3. The Correlation Characteristics and Energy Efficiency

3.1. Correlation Characteristics

Correlation characteristics [15] include the autocorrelation function and cross-correlation function. In the ultrasonic ranging system, the autocorrelation function of the *i*th echo sequence is defined as follows:

$$R_{ii}(m)=\begin{cases}\sum_{n=0}^{N-m-1}x_{n+m}^{i}x_{n}^{i} & m\geq 0\\ R_{ii}(-m) & m<0\end{cases}, i=1,2,\ldots,M, \quad (8)$$

Where M is the channel number of ultrasonic system, x_n^i and x_{n+m}^i are the *n*th and (*m*+*n*)th sampling data point of the *i*th echo sequence, respectively, *N* is the total number of samples in the echo sequence.

The definition of the cross-correlation function of the *i*th and *j*th echo sequences is given as follows:

$$R_{ij}(m)=\begin{cases}\sum_{n=0}^{N-m-1}x_{n+m}^{i}x_{n}^{j} & m\geq 0\\ R_{ij}(-m) & m<0\end{cases}, i=1,\ldots M, j=1,\ldots M, i\neq j \quad (9)$$

Where x_n^j is the *n*th sampling data point of the *j*th echo sequence.

The excitation sequences with better correlation characteristics, i.e., sharper autocorrelation and flatter cross-correlation, have better crosstalk rejection ability.

3.2. Energy Efficiency

Because the ultrasonic sensor has a band-pass spectrum, the excitation energy can be transmitted by the ultrasonic system when spectra of the excitation sequences match with that of the ultrasonic sensor. The spectrum of the triggered sequence which mismatches with that of the ultrasonic system can decrease the energy efficiency. The "energy efficiency" means the ratio between the energy of the echo and that of the excitation sequence [15].

The energy efficiency η is defined as:

$$\eta=\frac{E_R}{E_T}, \quad (10)$$

$$E_R=\frac{1}{R_R}\sum_{i=1}^{N}X_i^2, \quad (11)$$

$$E_T=\frac{1}{R_T}\sum_{i=1}^{N}Y_i^2, \quad (12)$$

Where E_T and E_R are the energies of the excitation and echo sequences, respectively; R_T and R_R are the equivalent resistance of the transmitting and receiving circuits, respectively; X_i

and Y_i are the *i*th sampling data of excitation and echo sequences, respectively; N is the number of samples.

Because R_T and R_R are different, the efficiency ratio ς expressed as follows is used to compare the energy efficiency of two excitation sequences:

$$\varsigma = \frac{\eta_1}{\eta_2}, \tag{13}$$

Where η_1 and η_2 are the energy efficiencies of two excitation sequences, respectively.

4. The Parameter Configuration Method of the Chaotic Binary Modulation Excitation Sequence

The spectrum of chaotic binary modulation sequence with square carrier wave is different with that of sinusoid carrier wave. The chaotic binary modulation sequence with square carrier wave has a direct-current component and harmonic components. To improve the energy efficiency of excitation sequence, the harmonic components with higher energy should be adjusted in the pass-band of the ultrasonic system, which can ensure the spectrum of excitation sequence matches with that of the ultrasonic system.

The power spectral density of the c-BASK excitation sequence is expressed as follows:

$$P_{\text{BASK}}(f) = \frac{T_s}{8}\left|\frac{\sin \pi f T_s}{\pi f T_s}\right|^2 + \frac{1}{8}\delta(f) + \sum_{k=0}^{\infty}\left\{\begin{array}{l}\frac{T_s}{8\pi(2k+1)}\left[\left|\frac{\sin\pi(f+(2k+1)f_c)T_s}{\pi(f+(2k+1)f_c)T_s}\right|^2 + \left|\frac{\sin\pi(f-(2k+1)f_c)T_s}{\pi(f-(2k+1)f_c)T_s}\right|^2\right] \\ + \frac{1}{8\pi(2k+1)}\left[\delta(f+(2k+1)f_c) + \delta(f-(2k+1)f_c)\right]\end{array}\right\} \tag{14}$$

And the power spectral density of the c-BPSK excitation sequence is the following:

$$P_{\text{BPSK}}(f) = \frac{1}{2} + \sum_{k=0}^{\infty}\left\{\frac{T_s}{2\pi(2k+1)}\left[\left|\frac{\sin\pi(f+(2k+1)f_c)T_s}{\pi(f+(2k+1)f_c)T_s}\right|^2 + \left|\frac{\sin\pi(f-(2k+1)f_c)T_s}{\pi(f-(2k+1)f_c)T_s}\right|^2\right]\right\} \tag{15}$$

From (14) and (15), we can find that the change tendency of amplitude among frequency range $[(2k+1)f_c - f_s, (2k+1)f_c + f_s]$ at different values of *k* is similar. The highest amplitude appears in frequency range $[f_c - f_s, f_c + f_s]$. In other words, the most energy of the c-BASK and c-BPSK sequences is focused in frequency range $[f_c - f_s, f_c + f_s]$. Therefore, the bandwidth of c-BASK and c-BPSK are about $B_{\text{BASK}} = B_{\text{BPSK}} \approx 2f_s = 2/T_s$.

For the c-BASK and c-BPSK excitation sequences, the carrier frequency f_c and bandwidth $B_{\text{BASK}} = B_{\text{BPSK}}$ are determined by the central frequency of the ultrasonic sensor and the symbol width of base-band signal T_s, respectively. The carrier frequency is set to the central frequency of the ultrasonic sensor generally. It is assumed that the symbol width is $T_s = n/f_c, n = 1,2,\cdots$, $B_{\text{sonar}} = B_{\text{BASK}} = B_{\text{BPSK}} \approx 2/T_s = 2f_c/n$, where B_{sonar} is the bandwidth of the ultrasonic sensor.

The power spectral density of the c-BFSK excitation sequence is given as follows:

$$P_{\text{BFSK}}(f) = \frac{1}{2} + \sum_{k=0}^{\infty}\left\{\begin{array}{l}\frac{T_s}{8\pi(2k+1)}\left[\left|\frac{\sin\pi(f+(2k+1)f_1)T_s}{\pi(f+(2k+1)f_1)T_s}\right|^2 + \left|\frac{\sin\pi(f-(2k+1)f_1)T_s}{\pi(f-(2k+1)f_1)T_s}\right|^2\right] \\ + \frac{T_s}{8\pi(2k+1)}\left[\left|\frac{\sin\pi(f+(2k+1)f_2)T_s}{\pi(f+(2k+1)f_2)T_s}\right|^2 + \left|\frac{\sin\pi(f-(2k+1)f_2)T_s}{\pi(f-(2k+1)f_2)T_s}\right|^2\right] \\ + \frac{1}{8\pi(2k+1)}\left[\delta(f+(2k+1)f_1) + \delta(f-(2k+1)f_1)\right] \\ + \frac{1}{8\pi(2k+1)}\left[\delta(f+(2k+1)f_2) + \delta(f-(2k+1)f_2)\right]\end{array}\right\} \tag{16}$$

To make most of the energy of the c-BFSK sequence to be focused in the frequency band of the ultrasonic sensor, the parameter settings are determined by the following formulas:

$$\begin{cases} (f_1+f_2)/2=f_c \\ |f_1-f_2|<f_s \\ |f_1-f_2|+2f_s \approx B_{\text{sonar}} \\ f_1=n_1/T_{s1}, f_2=n_2/T_{s2} \\ f_s=\min(1/T_{s1},1/T_{s2}) \end{cases}, \quad (17)$$

Where T_{s1} and T_{s2} are the symbol widths of the "1" and "0" symbols, respectively. Considering that the number of the square carriers should be integral within a symbol width, n_1 and n_2 are positive integers. Also, the symbol widths of the "1" and "0" are a little bit different.

5. The GA-based Optimization of the Chaotic Binary Modulation Excitation Sequence

Given the length of the chaotic binary modulation excitation sequence, symbol width and carrier frequency, a GA is used to optimize the chaotic initial values to get the best correlation characteristics (i.e., sharpest autocorrelation and flattest cross-correlation). The procedure is presented in the following steps.

Step 1: The initial parent population $A_{P\times Q}$ is produced randomly, where *P* is the population size and *Q* is the length of float chaotic initial values. Let *P* = 100, $Q=M$ (corresponding to M chaotic initial values for M channel ultrasonic system), and the maximum generation number is set to 100.

Step 2: The objective-function values of individuals are ordered and then mapped to fitness values. Then a column vector of fitness values is returned. An objective function $ObjV$ defined as follows:

$$ObjV := \max(R_{a\text{-max}}, R_{c\text{-max}}) \quad (18)$$

$$R_{a\text{-max}} := \max(R_{ii}(m)), i=1,\ldots,M, m=0,\ldots N-1-\delta \quad (19)$$

$$R_{c\text{-max}} := \max(R_{ij}(m)), m=0,1,2,\ldots 2N-1, i=1,\ldots M, j=1,\ldots M, i\neq j \quad (20)$$

Where $R_{a\text{-max}}$ is the maximal side-lobe among *M* autocorrelation functions, $R_{c-\max}$ is the maximal peak among $M(M-1)/2$ cross-correlation functions.

Step 3: The selection probability of individuals is set to 0.9, and the selected individuals are returned to the new population.

Step 4: The crossover and mutation operators are used to generate the new children population.

Step 5: The offspring population is combined with the current generation population and selection is performed to set the individuals for the next generation. Since all the previous and current best individuals are added to the population, elitism is ensured. Repeat Step 2 to Step 5 until the maximum generation number is reached.

6. Experiments and Discussion

6.1. Experimental Setup

The eight-channel ultrasonic ranging system was used in our experiments. Each channel of the ultrasonic ranging system has the same hardware realization. Figure 1 shows the hardware realization schematic diagram for one channel ultrasonic ranging system. The chaotic binary modulation sequence was sent from the field programming gate array (FPGA). After power amplifying, the ultrasonic sensor was triggered to transmit ultrasound. In our

experiments, a SensComp 600 series instrument-grade electrostatic sensor was used as both transmitter and receiver. After band-pass filtering, automatic gain amplification and shaping, the polarity correlation between the binary echo sequence and a reference echo sequence was carried out. The reference echo sequence was recoded from an acrylic board placed 40 cm in front of the ultrasonic sensor. Here it should be noted that the emitted pulse sequence and its echo sequence are different owing to the filtering effect of the ultrasonic sensor, so the correlation characteristics between the excitation sequence and its own echo is poor. That is why we did not use the emission sequence as the reference to calculate the correlation characteristics. Actually, similar correlation processing method was also adopted by Jörg *et al*. [17], where the echo instead of the emitted pulse sequence was used as the reference. Lastly, the distance calculation was implemented if the echo sequence was recognized to be from its own sensor transmission.

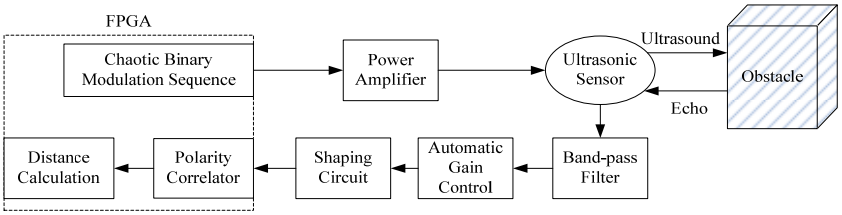

Figure 1. The hardware realization schematic diagram for one channel ultrasonic ranging system

6.2. The Spectrum of the Ultrasonic Ranging System

The purpose of this experiment is to figure out the usable frequency band of the Senscomp 600 electrostatic ultrasonic ranging system. In this experiment, each excitation sequence included ten 50%-duty-cycle rectangle pulses with same frequency. The frequency range was from 20 kHz to 100 kHz, the interval was 0.5 kHz. The excitation sequences were the binary sequences. Then all the corresponding echo sequences were sampled which reflected from an acrylic board placed 40 cm in front of ultrasonic sensor.

Through calculating the energies of the excitation sequences and echo sequences, the spectrum of the ultrasonic ranging system is shown in Figure 2. From this experiment, it can be found that ultrasonic ranging system has its own central frequency. The central frequency and the frequency band of the ultrasonic system are about 55 kHz and [40, 70] kHz, respectively. The nearer is the excitation sequence frequency to the central frequency, the less is the echo signal attenuation. The further is the excitation sequence frequency to the central frequency, the more is the echo signal attenuation.

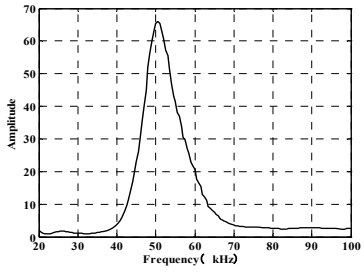

Figure 2. The Spectrum of the ultrasonic ranging system

6.3. Experimental Results and Discussion

For each chaotic binary modulation sequence, eight chaotic code series were used to construct eight channels of excitation sequences, respectively. The length of the chaotic binary modulation excitation sequence is set to 2 ms. Using the GA optimization algorithm, after 100 generations of selection, crossover and mutation, the optimized results for the c-BASK, c-BFSK

and c-BPSK sequences were $ObjV^{c}_{BASK} = 0.4735$, $ObjV^{c}_{BFSK} = 0.3379$ and $ObjV^{c}_{BPSK} = 0.3666$, respectively.

6.3.1. The Spectrum and Echo Analysis of Chaotic Binary Modulation Sequences

Figure 3(a), 4(a) and 5(a) show that the c-BASK, c-BPSK and c-BFSK excitation sequences when the chaotic initial values are optimized based on GA, respectively. In subfigures (b) of Figure 3-5, the black lines are the spectra of the chaotic binary modulation excitation sequences in Figure 3(a), 4(a) and 5(a), and the red lines are the spectrum of the ultrasonic ranging system. As shown in Figure 3(b), there is significant amount of spectral distributes in the frequency band [1, 40] kHz as well as in the frequency band [40, 70] kHz, which is the pass-band of the ultrasonic ranging system. In other words, the spectrum of c-BASK excitation sequence mismatches with that of the ultrasonic ranging system, the excitation energy in frequency band [1, 40] kHz cannot be transmitted by the ultrasonic system. Compared to the c-BASK, c-BPSK in Figure 4(b) presents that there is more spectral distributes in the pass-band of the ultrasonic ranging system (i.e., [40, 70] kHz), but some excitation energy is still in frequency band [1, 40] kHz which is not in the pass-band of the ultrasonic ranging system. As shown in Figure 5(b), there is more energy of c-BFSK sequence distributes in the frequency band of the ultrasonic ranging system than that of c-BASK and c-BPSK sequences, at the same time, there is less energy of c-BFSK sequence distributes in the out-band of the ultrasonic ranging system. Therefore, in three chaotic binary modulation excitation sequences, the c-BFSK excitation sequence most spectrally matches with the ultrasonic ranging system.

Figure 3(c), 4(c) and 5(c) illustrate the corresponding echo sequences of c-BASK, c-BPSK and c-BFSK excitation sequences, respectively. All the echo sequences were reflected from an obstacle placed 40 cm in front of the ultrasonic sensor. The sample period was $1\,\mu s$. The c-BFSK method in Figure 5c produces the highest echo amplitude of 0.9 V at some sampling time and most echo amplitude of [0.6, 0.8] V caused by the matched spectra between the excitation sequence and ultrasonic ranging system. As indicated in Figure 4(b) and 5(b), the echo amplitude in c-BASK and c-BPSK are less than that of the c-BFSK in Figure 3(b). Among three chaotic binary modulation sequences, the c-BFSK shows the best result, i.e., echo amplitude of 0.9 V due to excellent matching spectra between the excitation sequence and ultrasonic ranging system as shown in Figure 5(b).

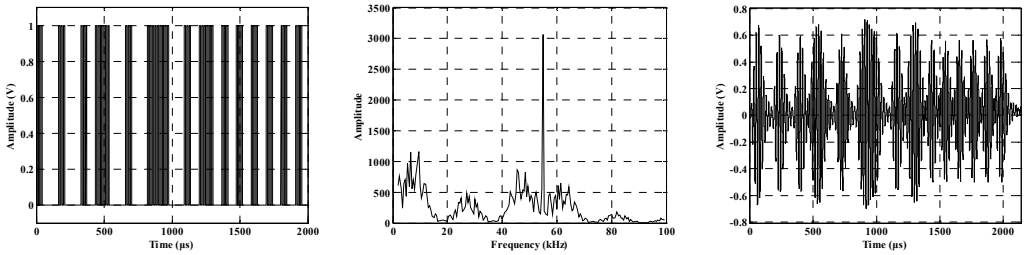

Figure 3. Optimized c-BASK sequence: (a) optimized c-BASK sequence, (b) the spectrum of (a), (c) the corresponding echo sequence

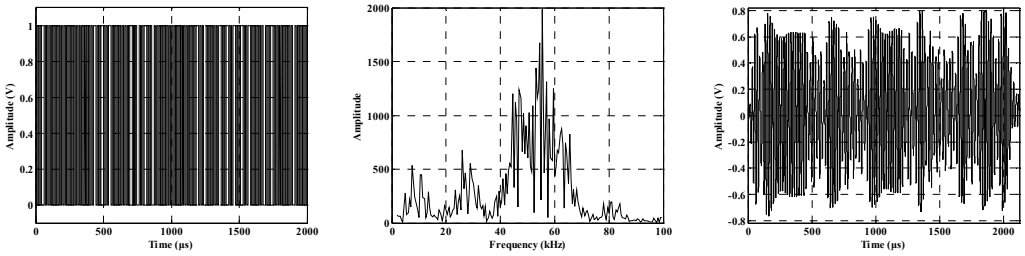

Figure 4. Optimized c-BPSK sequence: (a) optimized c-BPSK sequence, (b) the spectrum of (a), (c) the corresponding echo sequence

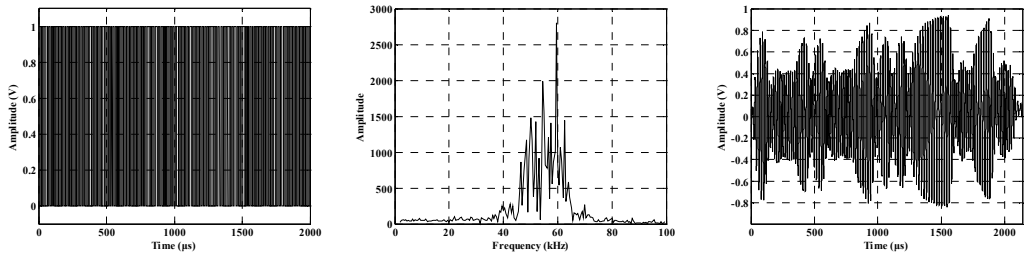

Figure 5. Optimized c-BFSK sequence: (a) optimized c-BFSK sequence, (b) the spectrum of (a), (c) the corresponding echo sequence

To quantitative comparison, the echo energies of the c-BASK, c-BFSK and c-BPSK excitation sequences corresponding to Figure 3-5 are listed in Table 1. From Table 1, we can see that the echo energy of the c-BFSK excitation signal is better than that of the c-BPSK and c-BASK signals. It can be also found that the energies of the three excitation sequences were different. Both the echo and the excitation energies of the c-BASK sequences are the smallest.

The energy efficiencies of the three chaotic binary modulation sequences are also calculated based Equation (10)-(13). The energy efficiencies of the c-BASK, c-BFSK and c-BPSK excitation sequences corresponding to Figure 3-5 are illustrated in Table 1. It can be found that the energy efficiency of the c-BFSK excitation sequence is better than that of the c-BPSK and c-BASK sequences.

Table1. The echo energies of c-BASK, c-BFSK and c-BPSK excitation sequences

Excitation Sequences	BASK	BFSK	BPSK
Excitation Sequences Energy ($V^2 \cdot \mu s$)	498.0000	1022.0000	1003.0000
Echo Energy ($V^2 \cdot \mu s$)	167.5800	358.4800	328.8600
Energy efficiency	0.3365 ς	0.3508 ς	0.3279 ς

6.3.2. The Correlation Characteristic Analysis of Chaotic Binary Modulation Sequences

Figure 6-7 show the correlation characteristic of c-BASK without optimization and after optimization, i.e., correlation characteristic includes the autocorrelation functions of two echo sequences and the crosscorrelation function. As shown in Figure 6-7, the optimized c-BASK sequences have lower side-lobe of echo autocorrelation functions than that of the unoptimized c-BASK sequences, i.e., 0.33 vs 0.58. Moreover, the c-BASK sequence after optimization also has lower peak of echo crosscorrelation function than that of the c-BASK sequence without optimization, i.e., 0.39 vs 0.51. The comparison results between the optimized c-BFSK sequences and the unoptimized c-BFSK sequences are presented in Figure 8-9. From these figures, we can find that the side-lobe of echo autocorrelation functions of the optimized c-BFSK sequences is about 0.14 lower than that of the unoptimized c-BFSK sequences. And the peak of echo crosscorrelation function of the optimized c-BFSK sequences is about 0.1 lower than that of the unoptimized c-BFSK sequences. Figures 10-11 demonstrate the correlation characteristic of c-BPSK without optimization and after optimization. As indicated in Figure 10-11, the side-lobe of echo autocorrelation functions of the optimized c-BPSK sequences is about 0.1 lower than that of the unoptimized c-BPSK sequences. And the peak of echo crosscorrelation function of the optimized c-BPSK sequences is about 0.08 lower than that of the unoptimized c-BPSK sequences.

Comparison with the optimized c-BASK and c-BPSK sequences, the correlation characteristic of the optimized c-BFSK sequence is lower than that of c-BASK and c-BPSK, i.e., the optimized c-BFSK sequence has the lowest side-lobe of echo autocorrelation functions and the lowest peak of echo crosscorrelation function. In other words, the optimized c-BFSK sequence has the best echo correlation characteristics among the chaotic binary modulation sequences.

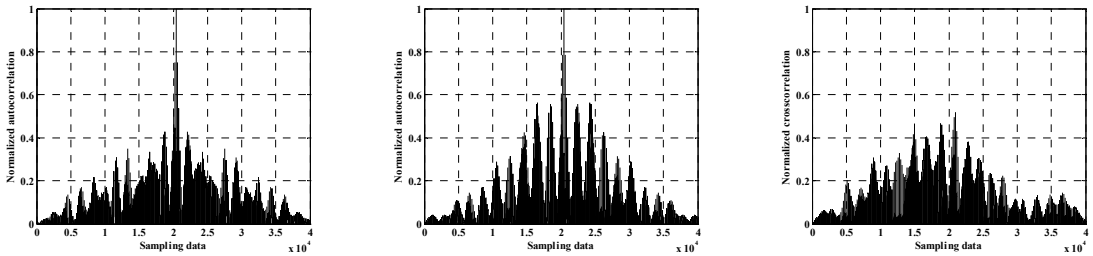

(a) (b) (c)

Figure 6. The correlation characteristic of c-BASK without optimization: (a) the normalized autocorrelation of echo sequence 1, (b) the normalized autocorrelation of echo sequence 2, (c) the normalized crosscorrelation of echo sequence 1 and 2

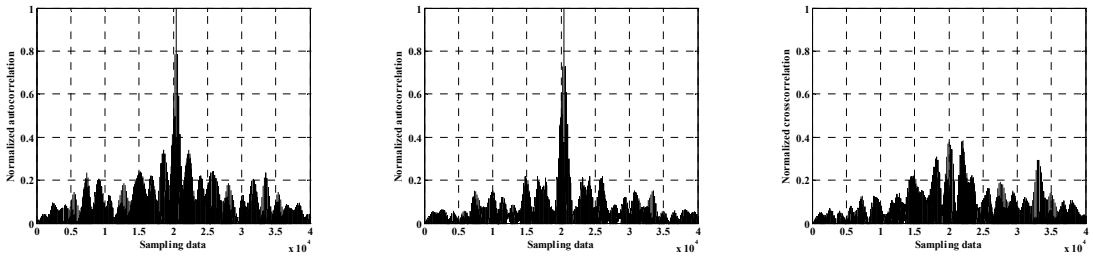

(a) (b) (c)

Figure 7. The correlation characteristic of c-BASK after optimization: (a) the normalized autocorrelation of echo sequence 1, (b) the normalized autocorrelation of echo sequence 2, (c) the normalized crosscorrelation of echo sequence 1 and 2

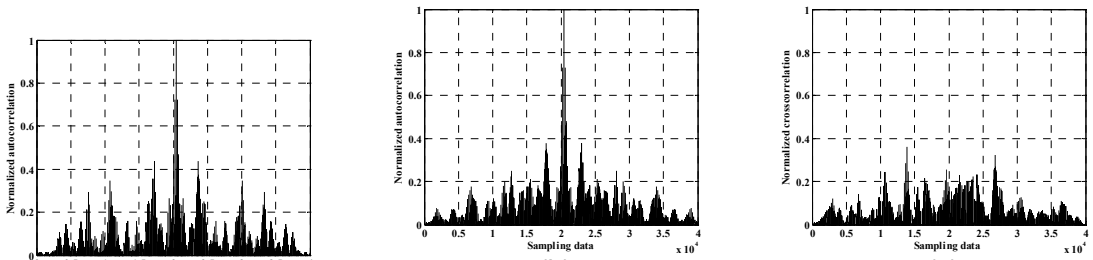

(a) (b) (c)

Figure 8. The correlation characteristic of c-BFSK without optimization: (a) the normalized autocorrelation of echo sequence 1, (b) the normalized autocorrelation of echo sequence 2, (c) the normalized crosscorrelation of echo sequence 1 and 2

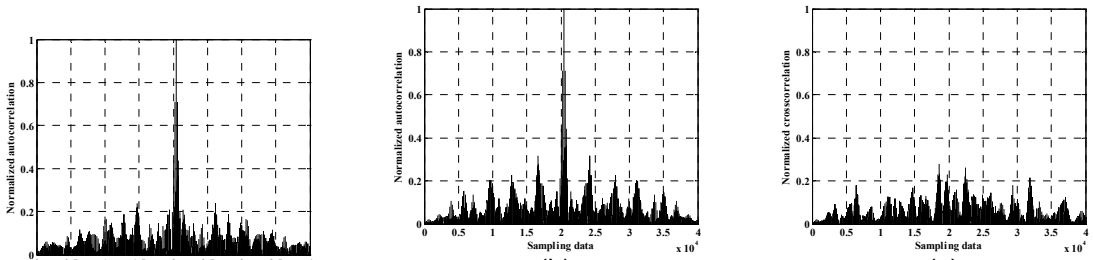

(a) (b) (c)

Figure 9. The correlation characteristic of c-BFSK after optimization: (a) the normalized autocorrelation of echo sequence 1, (b) the normalized autocorrelation of echo sequence 2, (c) the normalized crosscorrelation of echo sequence 1 and 2

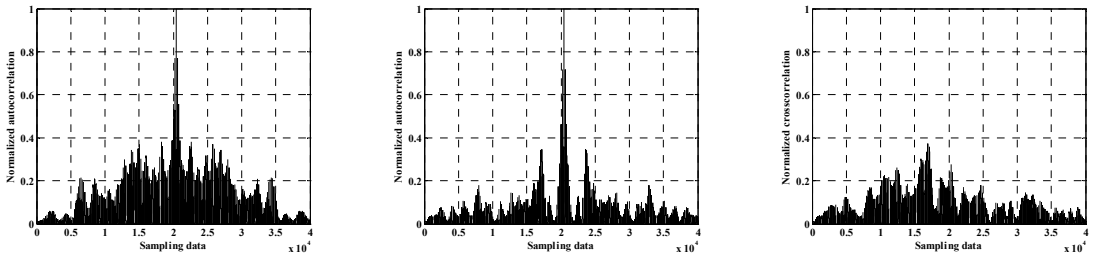

Figure 10. The correlation characteristic of c-BPSK without optimization: (a) the normalized autocorrelation of echo sequence 1, (b) the normalized autocorrelation of echo sequence 2, (c) the normalized crosscorrelation of echo sequence 1 and 2

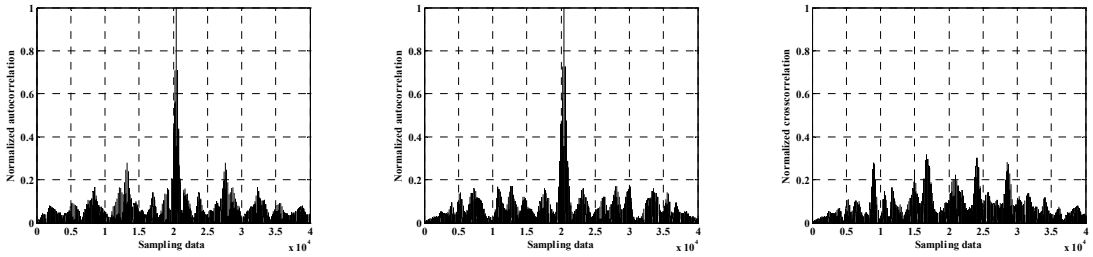

Figure 11. The correlation characteristic of c-BPSK after optimization: (a) the normalized autocorrelation of echo sequence 1, (b) the normalized autocorrelation of echo sequence 2, (c) the normalized crosscorrelation of echo sequence 1 and 2

7. Conclusion

In this paper, a crosstalk elimination method based on the optimal binary excitation sequences modulated with chaotic codes is presented in this paper. The parameters configuration method of the chaotic binary modulation sequence ensures the spectrum of excitation sequence matches with that of the ultrasonic ranging system, which improves the energy efficiency of excitation sequence. The optimized chaotic binary modulation sequence based GA has the best echo correlation characteristics. Experiments using an ultrasonic ranging system that consists of eight-channel SensComp 600 series instrument-grade electrostatic sensors excited with binary sequences showed that the c-BFSK outperforms the c-BASK and c-BPSK in terms of the energy efficiency, e.g., 0.3508ς vs. 0.3365ς and 0.3279ς, respectively. And the optimized c-BFSK sequence also has the best echo correlation characteristics among the chaotic binary modulation sequences.

Acknowledgements

The research work of this paper is sponsored by Teachers' Scientific Research Fund of China Earthquake Administration (No.20110121), Special Fund of Fundamental Scientific Research Business Expense for Higher School of Central Government (Projects for creation teams) (No. ZY20110104), the Seismic Technology Spark Plan Foundation of China (Grant No. XH12076), and National Natural Science Foundation of China (No. 60475028).

References

[1] H Moravec. Sensor fusion in certainty grids for mobile robots. AI Magazine. 1988; 9(2): 61-74.
[2] QH Meng, FJ Yao, YH Wu. *Review of crosstalk elimination methods for ultrasonic range systems in mobile robots*. Proceedings of IEEE/RSJ International Conference on Intelligent Robots and Systems. 2006: 1164-1169.

[3] KW Jörg, M Berg. Sophisticated mobile robot sonar sensing with pseudo-random codes. *Robotics and Autonomous Systems*. 1998; 25: 241-251.
[4] A Hernández, J Ureña, M Mazo, J García, A Jiménez, F Alvarez. Reduction of blind zone in ultrasonic transmitter/receiver transducers. *Sensors and Actuators*. 2007; 133: 96-103.
[5] A Hernández, J Ureña, D Hernanz, JJ García, M Mazo, JP Dérutin, J Sérot, SE Palazuelos. Real-time implementation of an efficient Golay correlator (EGC) applied to ultrasonic sensorial systems. *Microprocessors and Microsystems*. 2003; 27: 397-406.
[6] A Hernández, J Ureña, JJ García, M Mazo, D Hernanz, JP Dérutin, J Sérot. Ultrasonic ranging sensor using simultaneous emissions from different transducers. *IEEE Transactions on Ultrasonic, Ferroelectrics and Frequency Control*. 2004; 51(12): 1660-1670.
[7] ZX Ding, PA Payne. A new Golay code system for ultrasonic pulse echo measurements. *Measurement Science and Technology*. 1990; 1(2): 158-165.
[8] K Nakahira, S Okuma, T Kodama, T Furuhashi. *The use of binary coded frequency shift keyed signals for multiple user sonar ranging*. Proceedings of the IEEE International Conference on Networking, Sensing and Control. 2004: 1271-1275.
[9] F Alvarez, J Ureña, M Mazo, Á Hernández, J García, C Marziani. High reliability outdoor sonar prototype based on efficient signal coding. *IEEE Trans. Ultrason. Ferroelectr. Freq. Control.* 2006; 53(10): 1862-1871.
[10] H Iwasawa, J Takayama, S Ohyama. *A 3-D attitude measurement method using spread spectrum modulated ultrasonic wave.* Proceedings of SICE-ICASE International Joint Conference. 2006: 2802-2807.
[11] L Fortuna, M Frasca, A Rizzo. Chaotic pulse position modulation to improve the efficiency of sonar sensors. *IEEE Trans. Instrum. Meas.* 2003; 52(6): 1809–1814.
[12] ZJ Yao, QH Meng, GW Li, P Lin. *Non-crosstalk real-time ultrasonic range system with optimized chaotic pulse position-width modulation excitation*. Proceedings of 2008 IEEE Ultrasonics Symposium. 2008: 729-732.
[13] QH Meng, SY Lan, ZJ Yao, GW Li. Real-time noncrosstalk sonar system by short optimized pulse position modulation sequences. *IEEE Trans. Instrum. Meas*. 2009; 58(10): 3442-3449.
[14] M Pollakowski, H Ermert. Chirp signal matching and signal power optimization in pulse-echo mode ultrasonic nondestructive testing. I*EEE Trans. Ultrason. Ferroelectr. Freq. Control*. 1994; 41(5): 655-659.
[15] QH Meng, ZJ Yao, HY Peng. Improvement of energy efficiency via spectrum optimization of excitation sequence for multichannel simultaneously triggered airborne sonar system. *Rev. Sci. Instrum*. 2009; 80(12): 124903-1-124903-7.
[16] Y Jiang. On Ulam-von Neumann transformations. *Commun. Math. Phys.* 172(3) (1995) 449-459.
[17] K Jörg, M Berg. *Mobile robot sonar sensing with pseudo-random codes.* Proceedings of the 1998 IEEE International Conference on Robotics and Automation. 1998: 2807-2812.